



# Journal of Chemistry and Technologies

pISSN 2663-2934 (Print), ISSN 2663-2942 (Online).

journal homepage: <http://chemistry.dnu.dp.ua>

editorial e-mail: [chem.dnu@gmail.com](mailto:chem.dnu@gmail.com)



UDC 546.56:544:77:504.05

## GREEN SYNTHESIS OF TiO<sub>2</sub> NANOPARTICLES: A PROMISING TOOL FOR WASTEWATER TREATMENT

A. Zeenath Bazeera\*, Kairon Mubina M. S., S. M. Abdul Kader, M. Anisha Nashrin

Research Department of Physics, Sadakathullah Appa College (Autonomous), Affiliated to Manonmaniam Sundaranar University Tirunelveli, Tamil Nadu, India

Received 28 December 2024; accepted 20 February 2025; available online 15 July 2025

### Abstract

Non-biodegradable organic pollutants, such as textile dyes, pose significant risks to human health and the environment. Photocatalysis offers a sustainable and cost-effective solution for degrading these pollutants while simultaneously preventing microbial contamination. This study investigates the photocatalytic and antimicrobial activities of green TiO<sub>2</sub> NPs synthesized using an aqueous extract of *Allium sativum* (garlic). XRD analysis confirmed the anatase phase with an average crystallite size of 52 nm, while FTIR identified the characteristic Ti-O-Ti vibrational band at 470 cm<sup>-1</sup>. The NPs exhibited a band gap of 3.05 eV, UV absorbance at 337 nm, and a spherical morphology with slight agglomeration, as observed by FESEM. Antibacterial activity was demonstrated against *Streptococcus pneumoniae* and *Proteus vulgaris*, while antifungal activity was observed against *Aspergillus niger* and *Rhizopus sp.* Photocatalytic degradation achieved efficiencies of 78 % for Methylene Blue and 91 % for Rose Bengal, with kinetic rate constants of 0.008 min<sup>-1</sup> and 0.013 min<sup>-1</sup>, respectively. These findings highlight the potential of green TiO<sub>2</sub> NPs as a cost-effective approach for environmental remediation and microbial control.

Keywords: TiO<sub>2</sub> nanoparticles; *Allium sativum*; anti-bacterial; antifungal activity; Photodegradation; organic dyes.

## ЗЕЛЕНИЙ СИНТЕЗ НАНОЧАСТИНОК TiO<sub>2</sub> ЯК ПЕРСПЕКТИВНИЙ ІНСТРУМЕНТ ДЛЯ ОЧИЩЕННЯ СТИЧНИХ ВОД

А. Зенат Базіра, Кайрон Мубіна М. С., С. М. Абдул Кадер, М. Аніша Нашрін

Науково-дослідний відділ фізики, Автономний коледж Садакатхулла Аппа при університеті Манонманіам Сундаранар, Тірунелвелі, Таміл Наду, Індія

### Анотація

Органічні забруднювачі, що не розкладаються біологічно, такі як текстильні барвники, становлять значний ризик для здоров'я людини та навколишнього середовища. Фотокаталіз пропонує стійке та економічно ефективне рішення для деградації цих забруднювачів, одночасно запобігаючи мікробному забрудненню. У цій роботі досліджено фотокаталітичну та антимікробну активність зелених TiO<sub>2</sub> NPs, синтезованих з використанням водного екстракту часнику *Allium sativum* (часнику). Рентгеноструктурний аналіз підтвердив наявність фази анатазу з середнім розміром кристалітів 52 нм, а водночас ІЧ-спектроскопія ідентифікувала характерну коливальну смугу Ti-O-Ti за 470 см<sup>-1</sup>. За даними ФЕЕМ, наночастинки мали ширину забороненої зони 3.05 еВ, УФ-поглинання за 337 нм і сферичну морфологію з незначною агломерацією. Антибактеріальна активність була продемонстрована проти *Streptococcus pneumoniae* та *Proteus vulgaris*, протигрибкова активність спостерігалася проти *Aspergillus niger* та *Rhizopus sp.* Фотокаталітична деградація досягла ефективності 78 % для метиленового синього та 91 % для бенгальської троянди з кінетичними константами швидкості 0.008 хв<sup>-1</sup> та 0.013 хв<sup>-1</sup>, відповідно. Ці результати підкреслюють потенціал «зелених» наночастинок TiO<sub>2</sub> як економічно ефективного підходу до відновлення довкілля та боротьби з мікроорганізмами.

Ключові слова: Наночастинки TiO<sub>2</sub>; *Allium sativum*; антибактеріальна; протигрибкова активність; фотодеградація; органічні барвники.

\*Corresponding author: e-mail: [kaironmubinams@sadakath.ac.in](mailto:kaironmubinams@sadakath.ac.in)

© 2025 Oles Honchar Dnipro National University;

doi: 10.15421/jchemtech.v33i2.319532

## Introduction

Providing clean drinking water for all remains a significant global challenge. Water is essential for life, yet the increasing demand for clean water necessitates innovative technological solutions. The textile industry, particularly the dye sector, is a major contributor to water pollution, consuming vast amounts of water during dye processing [1]. Annually, approximately 700,000 tons of various dyes are produced globally, with over 15 % released into the environment through wastewater [2]. These dyes contribute to eutrophication, decreased oxygen levels, the circulation of carcinogenic agents, and numerous waterborne diseases. Consequently, eliminating synthetic dyes is critical, as their degradation by-products may also be carcinogenic, rendering biodegradation insufficient for treatment. Decolorizing dye effluent by removing dyes is thus an essential aspect of wastewater treatment, particularly in tanneries and the textile industry [3].

Various methods for dye removal from water bodies have been explored, including biological degradation, membrane filtration, adsorption, sedimentation, physical coagulation, and chemical coagulation. However, these methods are not entirely effective, as they often fail to degrade dye molecules, merely transforming them and potentially causing secondary pollution. This highlights the urgent need for advanced and efficient techniques to remove dyes and other organic pollutants from water. Advanced oxidation processes (AOPs) have emerged as promising alternatives for dye removal. These chemical processes generate hydroxyl radicals, highly reactive species capable of completely degrading organic pollutant molecules [4].

With the advancement of nanotechnology, nanoparticles have been successfully employed in wastewater treatment. Numerous studies highlight the significance of metal oxide nanoparticles as nontoxic antibacterial, antiviral, anticancer, and photocatalytic agents [5]. Among the various metal oxide nanoparticles, titanium dioxide ( $\text{TiO}_2$ ) is one of the most extensively studied due to its abundance, remarkable photocatalytic properties, chemical stability, and nontoxic nature. Titanium dioxide, a binary metal oxide, typically exists in two primary phases: rutile and anatase. Among its various applications, the photocatalytic activity of titanium dioxide nanoparticles stands out as particularly noteworthy. Photosensitizers, compounds capable of transferring energy to a reactant by

absorbing light in a photochemical reaction, form the basis for the degradation of pollutants through oxidation [6].

Currently, titanium dioxide nanoparticles are among the most widely used photocatalysts due to their low cost, excellent stability, high oxidation potential, strong catalytic activity, distinct antibacterial and antifungal properties, and nontoxicity [7]. Moreover, researchers have proposed that  $\text{TiO}_2$  nanoparticles can effectively inhibit fungal growth on biofilms, particularly those formed on medical devices. The impact of  $\text{TiO}_2$  nanoparticles on methicillin-resistant *Staphylococcus aureus* (MRSA) was specifically studied by Roy et al. in 2010 [8].

Numerous techniques, such as sol-gel, hydrothermal, solvothermal, flame combustion, emulsion precipitation, and fungus-mediated biosynthesis, have been explored for synthesizing  $\text{TiO}_2$  nanopowders. The fascinating interplay between inorganic nanoparticles and biological structures has made nanoscience and nanotechnology an exciting field of study. In recent years, the "green synthesis" of nanomaterials through environmentally friendly processes has gained significant attention. This approach involves utilizing prokaryotic or eukaryotic organisms (including bacteria, plants, and animals) or their components to produce metal and metal oxide nanoparticles. Among these, plant-derived nanoparticles are particularly suitable for biological applications due to the absence of toxic chemicals in their production process, and they offer faster synthesis compared to physicochemical methods [9].

Garlic (*Allium sativum*), a member of the Alliaceae family, is widely used and predominantly cultivated in Asia. Garlic contains water, proteins, carbohydrates, fats, fiber, sulfur compounds, vitamins, and minerals. Its bioactive components, such as allicin, saponins, phenols, and polysaccharides, contribute to its extensive health benefits. Allicin, produced when garlic cloves are crushed, exhibits antiviral, antibacterial, antifungal, antiparasitic, and anticancer properties [10]. Despite these biotherapeutic applications, the precise mechanisms underlying garlic's biological activity remain unclear, and relatively few studies have focused on synthesizing capped nanomaterials using garlic extract. Research on the green synthesis of metal oxide nanoparticles using garlic extract is still in its infancy.

Moreover, to the best of the authors' knowledge, no studies have investigated the use of

*Allium sativum* (garlic) extract in the synthesis of  $\text{TiO}_2$  nanoparticles and their subsequent assessment for photocatalytic activity and antifungal properties against *Aspergillus niger* and *Rhizopus* species. Consequently, this study aimed to synthesize  $\text{TiO}_2$  nanoparticles using garlic extract as a stabilizing and reducing agent. The photocatalytic activity of these green-synthesized  $\text{TiO}_2$  nanoparticles was evaluated using Methylene Blue (MB) and Rose Bengal (RB) as model dyes. Additionally, the kinetics of dye degradation were studied, and the antifungal activity against *Aspergillus niger* and *Rhizopus* species, as well as the antibacterial activity against *Streptococcus pneumoniae* and *Proteus vulgaris*, were investigated.

## Materials and Methods

### Materials

Titanium tetra-isopropoxide (TTIP,  $\text{Ti}[\text{OCH}(\text{CH}_3)_2]_4$ , 97 % purity) and ethanol (99 % purity) were purchased from Merck, India. No additional purification was necessary, as all chemicals and reagents used were of analytical grade. All glassware was thoroughly washed and dried prior to use. Deionized distilled water was used to prepare all solutions.

### Preparation of Garlic Extract

Fresh mountain garlic was purchased from a local organic market in Tirunelveli, Tamil Nadu,

India. The plant was air-dried to remove any remaining moisture after being thoroughly washed with deionized water (DIW) to eliminate dust particles. Thirty grams of garlic cloves were then crushed using a mortar and pestle after being cleaned with distilled water. After adding 60 mL of distilled water, the mixture was heated to 60 °C on a hotplate for one hour. The mixture was then filtered, and the aqueous extract was stored for later use.

### Green Synthesis of $\text{TiO}_2$ Nanoparticles Using Garlic Extract

A mixture was prepared by adding 30 mL of garlic extract to 15 mL of TTIP, with continuous stirring. To enhance the solubility of TTIP, 10 mL of ethanol was introduced into the solution. This mixture was then stirred continuously for 3 hours at 60 °C. During this process, the solution changed to a pale yellowish-white color, indicating the formation of  $\text{TiO}_2$  nanoparticles. The solution was then filtered to separate the precipitate, which was dried at 110 °C for 8 hours. The dried precipitate was subsequently calcined in a muffle furnace at 500 °C for 2 hours. The experimental procedure is shown in Figure 1. The resulting pure white  $\text{TiO}_2$  nanoparticles were then sent for further characterization.

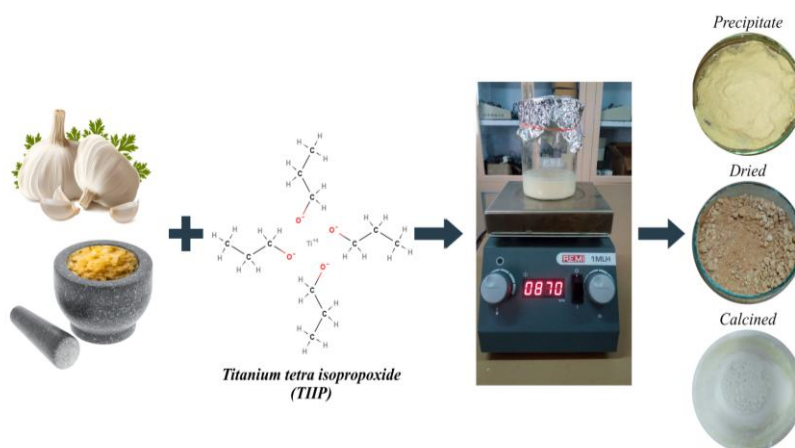


Fig. 1. Green synthesis of  $\text{TiO}_2$  nanoparticles using *Allium sativum*

### Characterization of $\text{TiO}_2$ Nanoparticles

The phase characteristics and crystalline structure of the green-synthesized  $\text{TiO}_2$  nanoparticles were analyzed using an X-ray diffractometer (X-Pert Pro) equipped with  $\text{Cu K}\alpha$  radiation (1.5405 Å). The instrument operated at 60 kV and 40 mA, with a  $2\theta$  range from 20° to 80°. Measurements were taken with a step size of 0.02 and a scanning rate of 5° per minute. FT-IR spectroscopy was used to examine the chemical bonding and functional groups of the synthesized

nanoparticles in the range of 4000–400  $\text{cm}^{-1}$  using a Perkin Elmer Model No. C-92107. The microstructure and surface morphology of the nanoparticles were observed using a Field Emission Scanning Electron Microscope (Model-Zeiss ULTRA 55). The UV-visible absorption spectrum of the green-synthesized  $\text{TiO}_2$  nanoparticles was recorded using an Agilent Technologies Cary 60 UV-visible spectrophotometer, with measurements taken in the range of 200 to 900 nm. Distilled water was

used as the reference solution for these measurements..

#### *In Vitro Antibacterial Activity*

The antibacterial activity of the green-synthesized  $\text{TiO}_2$  nanoparticles was evaluated against a Gram-positive bacterium, *Streptococcus pneumoniae*, and a Gram-negative bacterium, *Proteus vulgaris*, using the Kirby-Bauer method (Agar Disc Diffusion method). For the antibacterial assay, bacterial cells were grown in a broth culture. The media, along with the pipette, Petri dishes, and metallic borer, were sterilized in an autoclave at  $120^\circ\text{C}$  for 15 minutes. The culture media was then poured into Petri dishes under sterile conditions. The sample was dissolved in water to achieve a final concentration of  $20\text{ mg/mL}$ , and  $20\text{ }\mu\text{L}$  of the sample was loaded onto the discs. The antibacterial activity was analyzed by incubating the bacterial plates at  $37^\circ\text{C}$  for 24 hours.

#### *In Vitro Antifungal Activity*

The antifungal efficacy of the green-synthesized  $\text{TiO}_2$  nanoparticles was evaluated using the well diffusion method on Potato Dextrose Agar (PDA) medium. For each experiment, Petri dishes were prepared with PDA medium and inoculated with a fungal suspension of *Aspergillus niger* and *Rhizopus sp.*, with a

concentration of  $1000\text{ mL}$  and  $10^5\text{ CFU/mL}$ . The synthesized  $\text{TiO}_2$  nanoparticle sample was loaded onto the PDA plates. After inoculation, the plates were incubated at  $37^\circ\text{C}$  for three days. Following incubation, the zones of inhibition were carefully examined and analyzed.

#### *Photocatalytic Degradation Tests*

The photocatalytic degradation of Methylene Blue (MB) and Rose Bengal (RB) was performed using green-synthesized  $\text{TiO}_2$  nanoparticles. Twenty-five milligrams of the synthesized catalyst were mixed with  $25\text{ mL}$  of the dye solution. The mixture was then exposed to a  $400\text{ W}$  tungsten visible light lamp. The solution was stirred continuously until the reaction was complete. For the kinetic study of the degradation of MB and RB, a small aliquot of the dye solution containing the catalyst was taken at regular intervals and analyzed using UV-Vis spectroscopy. The reusability of the sample was tested by performing the photocatalytic degradation of the dyes three times under the same conditions. The catalyst was separated by centrifugation, washed with deionized water, and reused. UV-Vis spectra were collected in the range of  $300\text{--}800\text{ nm}$  using a UV-Vis spectrophotometer (Varian Cary 5000). The photocatalytic performance was calculated using the following expression [11]:

$$\text{Conversion efficiency (\%)} = \frac{C_0 - C_t}{C_0} \times 100,$$

where  $C_0$  and  $C_t$  are the initial and final concentrations of the aqueous dye solution, respectively. The Lagergren rate equation is widely used for the degradation of adsorbates from aqueous solutions. The Lagergren first-order model is represented as:

$$K = -\ln (C_t / C_0),$$

where  $K$  is the rate constant, and the kinetic rate constants are determined by plotting  $\ln (C_t/C_0)$  against irradiation time (min) [12].

## Results and Discussion

#### *XRD Analysis*

The X-ray diffraction (XRD) analysis reveals the crystalline structure of the green-synthesized titanium dioxide ( $\text{TiO}_2$ ) nanoparticles. Figure 2 shows the XRD pattern of the synthesized  $\text{TiO}_2$  nanoparticles.

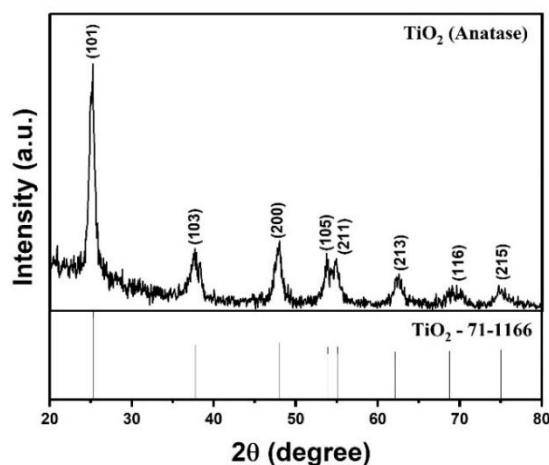


Fig. 2. XRD pattern of green synthesised  $\text{TiO}_2$  nanoparticles with standard JCPDS 71-1166 of  $\text{TiO}_2$

The pattern exhibits distinct peaks at  $2\theta$  values of  $25.04^\circ$ ,  $37.40^\circ$ ,  $47.83^\circ$ ,  $53.64^\circ$ ,  $54.81^\circ$ ,  $62.27^\circ$ ,  $68.99^\circ$ , and  $74.75^\circ$ . These peaks correspond to the (h k l) planes of (1 0 1), (1 0 3), (2 0 0), (1 0 5), (2 1 1), (2 1 3), (1 1 6), and (2 1 5), respectively. The observed values align well with the standard data provided in the JCPDS card No. 71-1166, confirming the formation of a tetragonal body-centered structure in the  $\text{TiO}_2$  nanoparticles. The lattice parameters were calculated to be  $a = b = 3.8028 \text{ \AA}$  and  $c = 9.6673 \text{ \AA}$  from the formula:

$$\frac{1}{d^2} = \frac{h^2 + k^2}{a^2} + \frac{l^2}{c^2},$$

where  $d$  is the d-spacing in  $\text{\AA}$ , and  $h$ ,  $k$ , and  $l$  are the Miller indices. The average crystalline size of the green-synthesized  $\text{TiO}_2$  nanoparticles was calculated from the XRD data using the Debye-Scherrer formula [13]:

$$D = \frac{k\lambda}{\beta \cos \theta},$$

where  $D$  is the crystalline size,  $k$  is a dimensionless shape factor (usually 0.9),  $\lambda$  is the wavelength of

the X-ray used ( $1.5406 \text{ \AA}$ ),  $\beta$  is the full-width at half-maximum intensity (FWHM), and  $\theta$  is the Bragg diffraction angle. The average crystalline size of the green-synthesized  $\text{TiO}_2$  nanoparticles was found to be approximately 52 nm. The average dislocation density was calculated using the formula:

$$\delta = \frac{1}{D^2},$$

where  $\delta$  is the dislocation density and  $D$  is the crystalline size of the nanoparticles. The average dislocation density was found to be  $6.19 \times 10^{15}$  lines per square meter. The high dislocation density indicates that the synthesized material has good yield strength and ductility. The microstrain was calculated using the formula [13]:

$$\epsilon = \frac{\beta}{4 \tan \theta},$$

where  $\epsilon$  is the microstrain and  $\beta$  is the FWHM value. The average microstrain was found to be 0.0064. The observed parameters are summarized in Table 1.

Table 1

XRD parameters of green synthesised $\text{TiO}_2$ nanoparticles		
S.No.	Parameters	Green Synthesized $\text{TiO}_2$ nanoparticles
1.	Lattice Parameter	
	• Standard	$a = b = 3.784 \text{ \AA}$ , $c = 9.514 \text{ \AA}$
	• Observed	$a = b = 3.8028 \text{ \AA}$ , $c = 9.6673 \text{ \AA}$
2.	Average Crystalline Size	52 nm
3.	Average Dislocation Density	$6.19 \cdot 10^{15}$ lines/ $\text{m}^2$
4.	Average Micro Strain	0.0064

The diffraction patterns of the samples reveal the predominant presence of titanium dioxide, with strong peaks clearly associated with the anatase phase. Additionally, the absence of any peaks related to impurities indicates a complete conversion of the titanium precursor into titanium dioxide ( $\text{TiO}_2$ ) nanoparticles. The sharpness and intensity of these diffraction peaks suggest that the nanoparticles have a well-defined crystalline structure. The high crystallinity of the  $\text{TiO}_2$  nanoparticles is further supported by the significant peak intensities. Thus, the XRD analysis affirms the effectiveness of garlic extract as a reducing agent in the synthesis of  $\text{TiO}_2$  nanoparticles.

#### FTIR Analysis

FT-IR spectroscopy was employed to identify potential biomolecules based on the chemical

groups present in *Allium sativum* extracts, which are summarized in Table 2. These biomolecules are responsible for capping and reducing metallic ions from the precursor, playing a critical role in nanoparticle synthesis. Figure 3 presents the FTIR spectrum, which was analyzed in the  $4000\text{--}400 \text{ cm}^{-1}$  range. The bands observed at  $3134$  and  $3011 \text{ cm}^{-1}$  correspond to the hydroxyl group (O-H stretching mode) present in polysaccharides and water [14]. The vibrational bands between  $2843$  and  $2360 \text{ cm}^{-1}$  correspond to the symmetric and anti-symmetric stretching of the methyl group ( $-\text{CH}_2$ ), predominantly originating from lipids [14; 15]. The band at  $1653 \text{ cm}^{-1}$  is associated with the carbonyl ( $\text{C=O}$ ) stretching, indicative of peptide linkages, which suggests the stretching of amides [16].

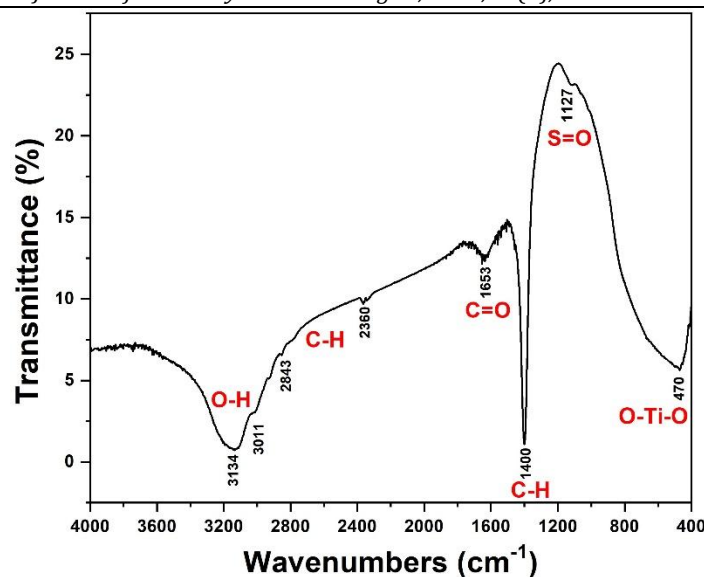


Fig. 3. FTIR spectra of green synthesised  $\text{TiO}_2$  nanoparticles

Moreover, the prominent peak at  $1400\text{ cm}^{-1}$  is attributed to the symmetric  $\text{CH}_3$  bending modes of methyl groups in proteins. This peak also implies the presence of flavonoids, tannins, saponins, and glycosides, as it represents the O-H bending of carboxylic acids [16; 17]. The peak at  $1127\text{ cm}^{-1}$  indicates the presence of the S=O group, suggesting the existence of organosulfur

compounds, such as alliin, allicin, and diallyl disulfide [17]. The stretching modes of Ti-O and Ti-O-Ti bridging are responsible for the broad range between  $800$  and  $400\text{ cm}^{-1}$  [14; 18]. The Ti-O bond vibration within the  $\text{TiO}_2$  (anatase titania) lattice is responsible for the peak at  $470\text{ cm}^{-1}$ , as observed in standard  $\text{TiO}_2$  spectra [19].

Table 2

FTIR tentative frequency assignment of green synthesised  $\text{TiO}_2$  nanoparticles

Wavenumber ( $\text{cm}^{-1}$ )	Band Assignment
3134 and 3011	Hydroxyl group (O-H stretching mode)
2800–2360	-CH <sub>2</sub> symmetric and anti-symmetric stretching of the methyl group
1653	Carbonyl and carboxylic (C=O) stretching bands
1400	Symmetric CH <sub>3</sub> bending modes
1127	S=O group / C-N stretching vibrations of primary amines
470	Ti-O-Ti bond

The FTIR results indicate the presence of proteins, as well as organosulfur compounds or aromatic amino acids on the surface of the nanoparticles. This interaction may result from the binding of proteins to nanoparticles, facilitated by free amine groups, cysteine residues, or through electrostatic attraction of negatively charged carboxylate groups. These mechanisms could play a role in the stabilization of  $\text{TiO}_2$  nanoparticles by proteins.

#### UV-Visible Spectral Analysis

The formation of  $\text{TiO}_2$  nanoparticles was initially assessed using UV-Vis spectroscopy. The UV absorption spectra of  $\text{TiO}_2$  nanoparticles, synthesized via a green method, are presented in Figure 4. The spectra show a prominent absorption band at  $337\text{ nm}$  within the  $200$ – $900$

nm range, with a determined band gap of  $3.05\text{ eV}$ , providing evidence for the successful green synthesis of  $\text{TiO}_2$  nanoparticles [19]. These findings are consistent with previous studies that used *Jatropha curcas* L. leaf extract for the synthesis of  $\text{TiO}_2$  nanoparticles [20]. Furthermore, the results suggest that  $\text{TiO}_2$ , when exposed to intense UV light, may function as a photocatalyst, facilitating the breakage of strong covalent bonds through the generation of hydroxyl radicals. The study highlights the role of active phytoconstituents in plant extracts in the stable synthesis of  $\text{TiO}_2$  nanoparticles, eliminating the need for toxic reducing chemicals, and demonstrating potential applications in various biological contexts.



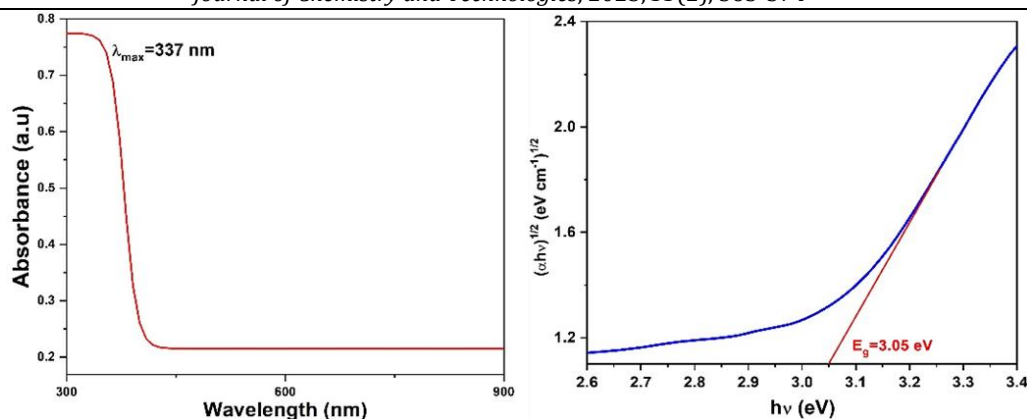


Fig. 4. UV-Vis. Spectra of green synthesised TiO<sub>2</sub> nanoparticles (a) absorption spectra (b) Tauc plot

#### FESEM and EDX Analysis

The morphology and size of the green-synthesized TiO<sub>2</sub> nanoparticles, using *Allium sativum* extract, were studied using Field Emission Scanning Electron Microscopy (FESEM) coupled with Energy-Dispersive X-ray (EDX) analysis, as shown in Figure 5 (a) and (b). The analysis revealed that the TiO<sub>2</sub> nanoparticles, predominantly in the anatase phase, are small and

spherical, with sizes ranging from 50 to 80 nm, as determined using ImageJ software. The EDX spectrum confirms the purity of the sample. These nanoparticles tend to agglomerate, a phenomenon attributed to the biomolecules adhering to their surfaces. These surface biomolecules attract additional molecules, primarily due to the electrostatic forces on the nanoparticle surfaces [21].

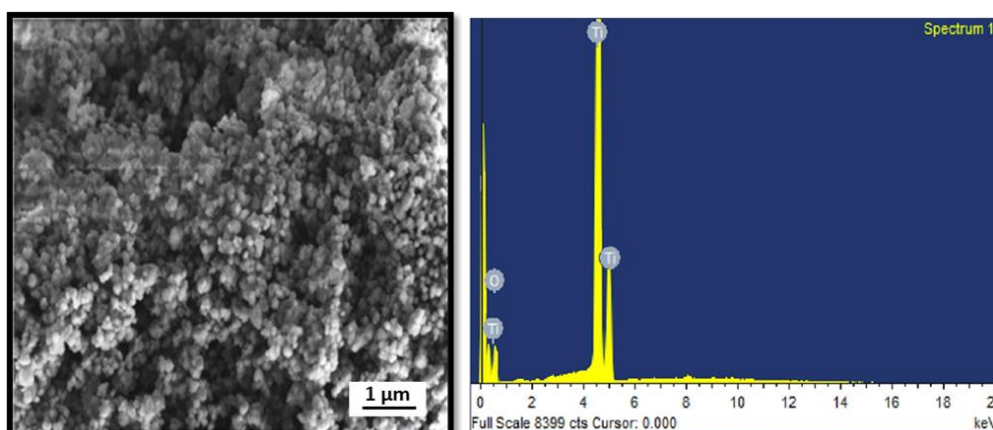


Fig. 5. (a) FESEM images (b) EDX spectra of green synthesised TiO<sub>2</sub> nanoparticles

#### In Vitro Antibacterial and Antifungal Activities of TiO<sub>2</sub> Nanoparticles

An additional objective was to assess the synthesized TiO<sub>2</sub> nanoparticles for their potential as antimicrobial agents, particularly those produced through green synthesis. Figure 6 (a) and (b) illustrate the inhibitory zones induced by TiO<sub>2</sub> nanoparticles against gram-positive and

gram-negative bacteria, respectively. The corresponding sizes of these inhibitory zones, in millimeters, are detailed in Table 3. Notably, TiO<sub>2</sub> nanoparticles exhibit significant antibacterial activity, as evidenced by the maximum inhibition zones of 22.5 mm against *Streptococcus pneumoniae* and 21.4 mm against the gram-negative bacterium *Proteus vulgaris*.

Table 3

Antibacterial and Antifungal activity of green synthesized TiO <sub>2</sub> nanoparticles			
S.No.	Pathogen Name	Zone of Inhibitions (mm)	
		Control	TiO <sub>2</sub>
Bacteria			
1.	<i>Streptococcus pneumoniae</i> (gram positive)	0	22.5
2.	<i>Proteus vulgaris</i> (gram negative)	0	21.4
Fungus			
1.	<i>Aspergillus niger</i>	0	19.8
2.	<i>Rhizopus sp.</i>	0	27.8

The bactericidal effect of TiO<sub>2</sub> nanoparticles is primarily attributed to the degradation of bacterial outer membranes by reactive oxygen species (ROS), particularly hydroxyl radicals ( $\bullet\text{OH}$ ) [22]. This process, driven by photocatalytic oxidation reactions initiated by absorbed photons, generates positive holes ( $\text{h}^+$ ) and negative electrons ( $\text{e}^-$ ) in the TiO<sub>2</sub> catalyst. The hydroxyl radicals formed during this process contribute to phospholipid peroxidation, ultimately leading to cell death [23; 24]. The nanoparticles also interact physically with bacterial cell walls, causing damage and initiating an oxidative stress environment. This oxidative stress, including the production of H<sub>2</sub>O<sub>2</sub>, affects mitochondrial enzymes and proteins, leading to changes in macromolecules such as proteins, nucleic acids, and lipids. The resulting ROS induce free radicals that influence nuclear viability, impair the cell membrane, alter permeability, and inhibit metabolic processes, all contributing to the

antibacterial activity of TiO<sub>2</sub> nanoparticles. Green-synthesized TiO<sub>2</sub> nanoparticles from *Allium sativum* demonstrated excellent antibacterial activity against both gram-positive and gram-negative bacteria.

Nevertheless, Figures 6 (c) and (d) demonstrate the notable antifungal efficacy of the green-synthesized TiO<sub>2</sub> nanoparticles against *Aspergillus niger* and *Rhizopus* sp. at a concentration of 10<sup>5</sup> CFU/ml. Exposure to the nanoparticles led to various alterations in the structure of the fungal cell walls. These changes included surface contraction, clustering of cells, and the formation of pits, pores, and overall shape distortion. Reactive oxygen species (ROS) play a crucial role in this process by contributing to lipid peroxidation, which can damage the cell wall. Specifically, titanium dioxide nanoparticles are efficient at absorbing light and generating ROS, primarily hydroxyl radicals.

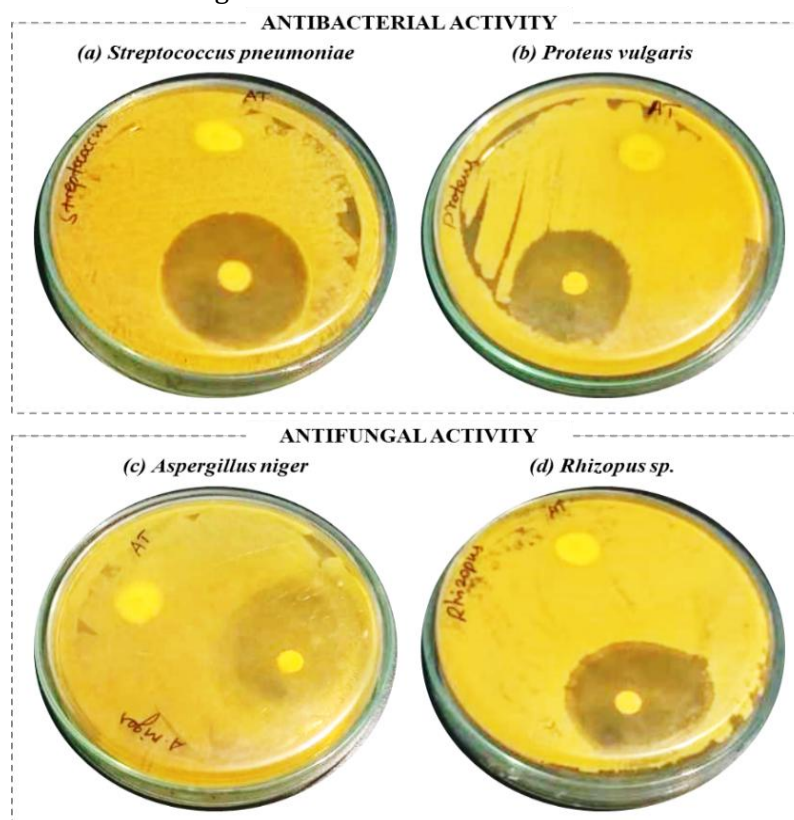


Fig. 6. Antibacterial and Antifungal activity of green synthesized TiO<sub>2</sub> nanoparticles (a) *Streptococcus pneumoniae* (b) *Proteus vulgaris* (c) *Aspergillus niger* (d) *Rhizopus* sp.

These radicals target the monomers in the cell wall, breaking down the glycosidic bonds and forming pores, which ultimately lead to the death of the fungus [26]. Furthermore, the ROS generated by ions released from the nanoparticles in an oxidative environment deplete thiol levels, disrupting the internal redox balance and causing rupture of the cell membrane. The findings

highlight the harmful nature of TiO<sub>2</sub> nanoparticles for the tested bacterial and fungal strains, indicating their promising potential for use in commercial and medical applications as antibacterial and antifungal agents.

#### Photocatalytic Activity

Dyes are widely used in industries such as textiles, leather, paper, and cosmetics, but their



improper disposal causes significant environmental pollution. Among these, synthetic dyes like Methylene Blue and Rose Bengal are of particular concern due to their persistence and toxicity. These dyes are often discharged into water bodies, where they negatively impact aquatic ecosystems and human health.

Methylene Blue, a cationic dye, is commonly used in textiles, medicine, and as a biological stain. When released untreated, it contaminates water and poses risks to aquatic life. It can inhibit photosynthesis in aquatic plants by blocking sunlight penetration and disrupt ecosystem

balance. Prolonged exposure to Methylene Blue can lead to skin irritation, respiratory issues, and cytotoxic effects in humans [27].

Similarly, Rose Bengal, an organic dye with applications in diagnostics and staining, is known for its toxicity. It generates reactive oxygen species under light exposure, leading to oxidative stress in living organisms. When released into the environment, Rose Bengal can damage the cell structures of aquatic organisms and adversely affect ecosystems by promoting algae blooms, which deplete oxygen in water [28].

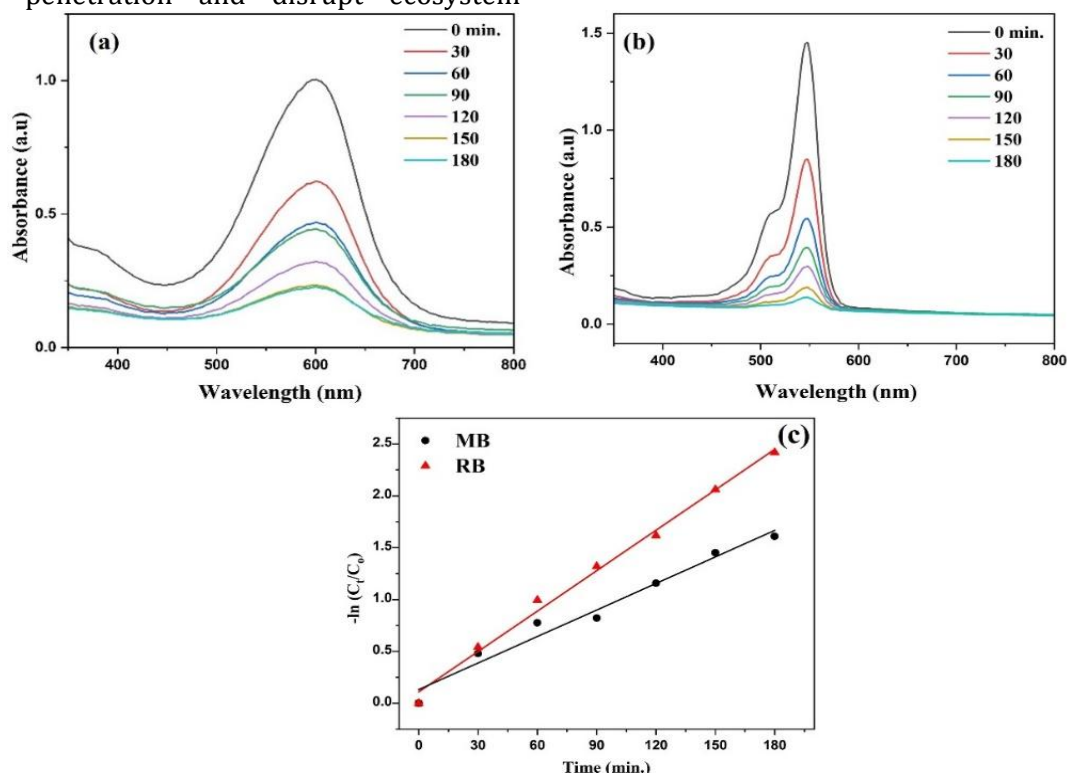


Fig. 7. (a & b) UV-Vis spectra of the green synthesized TiO<sub>2</sub> catalyst dispersed in Methylene Blue (MB) and Rose Bengal (RB) dye solution with light irradiation of different time interval, respectively, (c) Plot of  $-\ln(C_t/C_0)$  versus time interval

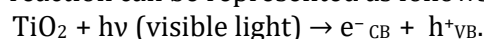
Table 4

Photocatalytic activity of green synthesized TiO <sub>2</sub> nanoparticles				
S.No.	Organic Dyes	Degradation efficiency (%)	Kinetic Constant (K, min <sup>-1</sup> )	R <sup>2</sup>
1.	Methylene Blue (MB)	78	0.0082	0.9601
2.	Rose Bengal (RB)	91	0.0132	0.9929

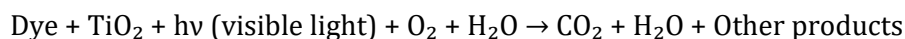
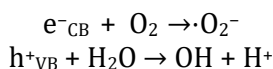
Since TiO<sub>2</sub> is a semiconductor, photons with sufficient energy can create electron-hole pairs. Light absorption by the TiO<sub>2</sub> nanoparticles causes electrons in the valence band to migrate to the conduction band, leaving behind holes in the valence band. The conduction band-activated electrons and valence band holes react with oxygen and ambient water to produce superoxide ions, hydroxyl radicals, and reactive oxygen species (ROS). These radicals, known for their high reactivity, can quickly damage organic substances

when they come into contact with them. When TiO<sub>2</sub> nanocatalysts are dispersed in the dye solution and exposed to visible light, TiO<sub>2</sub> absorbs photons, exciting electrons from the valence band (VB) to the conduction band (CB). This results in the formation of electron-hole pairs. Any pollutant deposited on the photocatalyst surface will be either reduced or oxidized due to the reactions of these pairs [11; 29; 30].

The reaction can be represented as follows:



The photogenerated electrons ( $e^-$  (CB)) and holes ( $h^+$  (VB)) react with oxygen ( $O_2$ ) and water ( $H_2O$ ) to form reactive oxygen species such as hydroxyl radicals ( $\cdot OH$ ) and superoxide anions ( $\cdot O_2^-$ ):



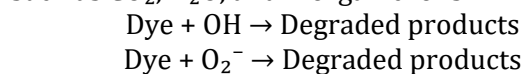
The degradation efficiency and the pseudo-first-order kinetic model parameters, along with the experimental values of the rate constant ( $K$ ) and  $R^2$ , are presented in Table 4. Figure 7 (a & b) depicts the UV-Vis spectra of the green-synthesized  $TiO_2$  catalyst dispersed in Methylene Blue (MB) and Rose Bengal (RB) dye solutions under light irradiation at different time intervals, respectively. The observed degradation efficiencies were 78 % for Methylene Blue (MB) and 91 % for Rose Bengal (RB). The kinetic rate constants for the photocatalytic degradation of MB and RB dyes using green-synthesized  $TiO_2$  nanoparticles were calculated to be  $0.008 \text{ min}^{-1}$  and  $0.013 \text{ min}^{-1}$ , respectively. The higher photocatalytic performance of  $TiO_2$  nanoparticles for RB degradation compared to MB is attributed to structural differences between the dyes. Rose Bengal, a halogenated xanthene dye, absorbs visible light more effectively. In contrast, Methylene Blue, a heterocyclic dye with a simpler aromatic structure, requires more energy to break its chemical bonds, making it less reactive to reactive oxygen species (ROS).

This study underscores the potential of green-synthesized  $TiO_2$  nanoparticles as efficient photocatalysts for degrading environmental pollutants. The superior catalytic activity for Rose Bengal compared to Methylene Blue demonstrates the promise of these nanoparticles in providing sustainable solutions to mitigate dye-induced environmental pollution.

## Conclusion

An environmentally friendly method was employed to synthesize  $TiO_2$  nanoparticles using an aqueous extract of *Allium sativum* (garlic) as a stabilizing agent. Comprehensive characterization techniques, including X-ray diffraction (XRD), Fourier Transform Infrared (FTIR) spectroscopy, ultraviolet-visible (UV-Vis) spectroscopy, and Field Emission Scanning Electron Microscopy (FESEM), confirmed the successful synthesis of the nanoparticles. XRD analysis confirmed the anatase phase with an average crystalline size of 52 nm. FTIR spectra identified characteristic

bands of allicin, a potent bioactive compound in garlic, at  $1127 \text{ cm}^{-1}$ , and the Ti-O-Ti vibration band at  $470 \text{ cm}^{-1}$ , indicating the involvement of garlic-derived phytochemicals in the nanoparticle formation process. UV-Vis spectroscopy revealed the optical properties of the nanoparticles, with a peak absorbance at 337 nm and a calculated bandgap of 3.05 eV from Tauc plot analysis. FESEM imaging demonstrated the formation of spherical nanoparticles with an average size ranging from 50 to 80 nm.



The overall reaction is:

bands of allicin, a potent bioactive compound in garlic, at  $1127 \text{ cm}^{-1}$ , and the Ti-O-Ti vibration band at  $470 \text{ cm}^{-1}$ , indicating the involvement of garlic-derived phytochemicals in the nanoparticle formation process. UV-Vis spectroscopy revealed the optical properties of the nanoparticles, with a peak absorbance at 337 nm and a calculated bandgap of 3.05 eV from Tauc plot analysis. FESEM imaging demonstrated the formation of spherical nanoparticles with an average size ranging from 50 to 80 nm.

The synthesized nanoparticles exhibited pronounced antibacterial and antifungal activities, attributed to the synergistic antimicrobial properties of both  $TiO_2$  and garlic. The photocatalytic performance of the nanoparticles was evaluated through the degradation of the organic dyes Methylene Blue (MB) and Rose Bengal (RB) under visible light irradiation. Degradation efficiencies of 78 % for MB and 91 % for RB were achieved, with kinetic rate constants of  $0.008 \text{ min}^{-1}$  and  $0.013 \text{ min}^{-1}$ , respectively.

These findings highlight the efficacy of green-synthesized  $TiO_2$  nanoparticles in the degradation of recalcitrant organic pollutants, demonstrating their promising potential for environmental remediation. Furthermore, their antimicrobial properties underscore their multifunctionality, providing a sustainable approach to water purification.

Thus, these environmentally friendly  $TiO_2$  nanoparticles exhibit substantial potential for large-scale applications in the future, particularly in the complete degradation of hazardous dyes from contaminated water, contributing to the advancement of sustainable environmental technologies.

## Data availability

The data that has been used is confidential.

## Acknowledgement

We sincerely thank Sadakathullah Appa College, Tirunelveli for providing the research facilities. We extend our gratitude to Manonmaniam Sundaranar University, Tirunelveli for their support. We would also like to

thank Alagappa University, Karaikudi (TN), Karunya Institute of Technology and Sciences, Coimbatore (TN), Sathyabama Institute of Science

and Technology, Chennai (TN) and Smykon Biotech, Nagercoil (TN) for their timely assistance with characterization.

## References

- [1] Kovács, I., Veréb, G., Kertész, S., Hodúr, C. and László, Z., (2018). Fouling mitigation and cleanability of TiO<sub>2</sub> photocatalyst-modified PVDF membranes during ultrafiltration of model oily wastewater with different salt contents. *Environmental Science and Pollution Research*, 25, 34912–34921. <https://doi.org/10.1007/s11356-017-0998-7>
- [2] Ambade, B., Kumar, A., Gautam, S. (2024). Sustainable solutions: reviewing the future of textile dye contaminant removal with emerging biological treatments. *Limnological Review*, 24(2), 126. <https://doi.org/10.3390/limnolrev24020007>
- [3] Kistan, A., Kanchana, V., Sakayasheela, L., Sumathi, J., Premkumar, A., Selvam, A. (2018). Titanium dioxide as a Catalyst for Photodegradation of Various Concentrations of Methyl Orange and Methyl Red dyes using Hg Vapour Lamp with Constant pH. *Oriental Journal of Chemistry*, 34(2). <http://dx.doi.org/10.13005/ojc/340250>
- [4] Ul Haq, A., Saeed, M., Khan, S.G. and Ibrahim, M. (2021). Photocatalytic applications of titanium dioxide (TiO<sub>2</sub>). *Titanium Dioxide-Advances and Applications*, 63–84.
- [5] Ahmad, W., Kalra, D. (2020). Green synthesis, characterization and anti microbial activities of ZnO nanoparticles using Euphorbia hirta leaf extract. *Journal of King Saud University-Science*, 32(4), 2358–2364. <https://doi.org/10.1016/j.jksus.2020.03.014>
- [6] Ahmad, W., Singh, A., Jaiswal, K.K., Gupta, P. (2021). Green synthesis of photocatalytic TiO<sub>2</sub> nanoparticles for potential application in photochemical degradation of ornidazole. *Journal of Inorganic and Organometallic Polymers and Materials*, 31, 614–623. <https://doi.org/10.1007/s10904-020-01703-6>
- [7] Khashan, Kh. S., Ghassan, M., Sulaiman, F. A. A., Salim Albukhaty, M. A. I., Al-Muhimeed, T., AlObaid, A. A. (2021). Antibacterial activity of TiO<sub>2</sub> nanoparticles prepared by one-step laser ablation in liquid. *Applied Sciences*, 11(10), 4623. <https://doi.org/10.3390/app11104623>
- [8] Yaqoob, A. A., Ahmad, H., Parveen, T., Ahmad, A., Oves, M., Ismail, I. M. I., Qari, H. A., Umar, K., Mohamad Ibrahim, M.N. (2020). Recent advances in metal decorated nanomaterials and their various biological applications: A review. *Front Chem.*, 8, 1–23. <https://doi.org/10.3389/fchem.2020.00341>
- [9] Singh, J., Dutta, T., Kim, K.-H., Rawat, M., Samddar, P., Kumar, P. (2018). Green' synthesis of metals and their oxide nanoparticles: applications for environmental remediation. *Journal of nanobiotechnology*, 16(1), 1–24. <https://doi.org/10.1186/s12951-018-0408-4>
- [10] Vijayakumar, S., Malaikozhundan B., Saravanakumar, K., Durán-Lara, E. F., Wang, M.-H., Vaseeharan, B. (2019). Garlic clove extract assisted silver nanoparticle–Antibacterial, antibiofilm, antihelminthic, anti-inflammatory, anticancer and ecotoxicity assessment. *Journal of Photochemistry and Photobiology B: Biology*, 198, 111558. <https://doi.org/10.1016/j.jphotobiol.2019.111558>
- [11] Lee, S. Y., Dooho, K., Sehee, J., Hoang, T. D., Joon, H. K. (2020). Photocatalytic degradation of rhodamine B dye by TiO<sub>2</sub> and gold nanoparticles supported on a floating porous polydimethylsiloxane sponge under ultraviolet and visible light irradiation. *ACS omega*, 5(8), 4233–4241. <https://doi.org/10.1021/acsomega.9b04127>
- [12] Murugadoss, G., Kumar, D.D., Kumar, M.R., Venkatesh, N., Sakthivel, P. (2021). Silver decorated CeO<sub>2</sub> nanoparticles for rapid photocatalytic degradation of textile rose bengal dye. *Scientific Reports*, 11(1), 1080. <https://doi.org/10.1038/s41598-020-79993-6>
- [13] Sundaram, P., Shunmuga, T., Sangeetha, S., Rajakarthishan, R., Vijayalaksmi, A., Elangovan, G. Arivazhagan. (2020). XRD structural studies on cobalt doped zinc oxide nanoparticles synthesized by coprecipitation method: Williamson-Hall and size-strain plot approaches. *Physica B: Condensed Matter*, 595, 412342. <https://doi.org/10.1016/j.physb.2020.412342>
- [14] Bagheri, S., Kamyar Sh., Abd Hamid, Sh. B. (2013). Synthesis and characterization of anatase titanium dioxide nanoparticles using egg white solution via sol-gel method. *Journal of Chemistry*, 2013. <http://dx.doi.org/10.1155/2013/848205>
- [15] Jalali, E., Maghsoudi, Sh., Noroozian, E. (2020). A novel method for biosynthesis of different polymorphs of TiO<sub>2</sub> nanoparticles as a protector for *Bacillus thuringiensis* from Ultra Violet. *Scientific Reports*, 10(1), 426. <https://doi.org/10.1038/s41598-019-57407-6>
- [16] Rastogi, L., Arunachalam, J. (2012). Microwave-assisted green synthesis of small gold nanoparticles using aqueous garlic (*Allium sativum*) extract: their application as antibiotic carriers. *International Journal of Green Nanotechnology*, 4(2), 163–173. <https://doi.org/10.1080/19430892.2012.676926>
- [17] Akilan, S., Prabakar, K. (2018). Spectral studies and antibacterial activity of Garlic (*Allium sativum* L.). *Journal of Emerging Technologies and Innovative Research*, 5(7), 452–457.
- [18] Saravanan, S., Dubey, R. S. (2021). Optical and morphological studies of TiO<sub>2</sub> nanoparticles prepared by sol-gel method. *Materials Today: Proceedings*, 47, 1811–1814, <https://doi.org/10.1016/j.matpr.2021.03.207>
- [19] Praveen, P., Viruthagiri, G., Mugundan, S., Shanmugam, N. (2014). Structural, optical and morphological analyses of pristine titanium di-oxide nanoparticles–Synthesized via sol-gel route. *Spectrochimica Acta Part A: Molecular and Biomolecular Spectroscopy*, 117, 622–629. <http://dx.doi.org/10.1016/j.saa.2013.09.037>
- [20] Goutam, S. P., Saxena, G., Singh, V., Yadav, A. K., Bharagava, R. N., Thapa, K. B (2018). Green synthesis of TiO<sub>2</sub> nanoparticles using leaf extract of *Jatropha curcas* L. for photocatalytic degradation of tannery wastewater. *Chemical Engineering Journal*, 336, 386–396. <https://doi.org/10.1016/j.cej.2017.12.029>
- [21] Shanavas, S., Priyadharsan, A., Karthikeyan, S., Dharmaboopathi, K., Ragavan, I., Vidya, C., Acevedo, R., Anbarasana, P. M. (2020). Green synthesis of titanium dioxide nanoparticles using *Phyllanthus niruri* leaf extract and study on its structural, optical and morphological properties. *Materials Today: Proceedings*, 26, 3531–3534. <https://doi.org/10.1016/j.matpr.2019.06.715>

- [22] Maryani, E., Nurjanah, N. S., Hadisantoso, E. P., Wijayanti, R. B. (2020). The Effect of TiO<sub>2</sub> additives on the antibacterial properties (*Escherichia coli* and *Staphylococcus aureus*) of glaze on ceramic tiles. In *IOP Conference Series: Materials Science and Engineering*, 980(1), 012011. <https://doi.org/10.1088/1757-899X/980/1/012011>
- [23] Rajakumar, G., Rahuman, A.A., Roopan, S. M., Gopiesh, V., Khanna, G. E., Kamaraj, C., Zahir, A. A., Velayutham, K. (2012). Fungus-mediated biosynthesis and characterization of TiO<sub>2</sub> nanoparticles and their activity against pathogenic bacteria. *Spectrochimica Acta Part A: Molecular and Biomolecular Spectroscopy*, 91, 23–29. <https://doi.org/10.1016/j.saa.2012.01.011>
- [24] Priyanka, K. P., Sukirtha, T. H., Balakrishna, K. M., Varghese, T. (2016). Microbicidal activity of TiO<sub>2</sub> nanoparticles synthesised by sol-gel method. *IET nanobiotechnology*, 10(2), 81–86. <https://doi.org/10.1049/iet-nbt.2015.0038>
- [25] Bahjat, H. H., Ismail, R. A., Sulaiman, G. M., Jabir, M. S. (2021). Magnetic field-assisted laser ablation of titanium dioxide nanoparticles in water for antibacterial applications. *Journal of Inorganic and Organometallic Polymers and Materials*, 31, 3649–3656. <https://doi.org/10.1007/s10904-021-01973-8>
- [26] Slavin, Y. N., Bach, H. (2022). Mechanisms of Antifungal Properties of Metal Nanoparticles. *Nanomaterials*, 12(24), 4470. <https://doi.org/10.3390/nano12244470>
- [27] Gupta, V. K. (2009). Application of low-cost adsorbents for dye removal—a review. *Journal of environmental management*, 90(8), 2313–2342. [10.1016/j.jenvman.2008.11.017](https://doi.org/10.1016/j.jenvman.2008.11.017)
- [28] Hassan, M. G., Wassel, M. A., Gomaa, H. A., Elfeky, A. S. (2023). Adsorption of Rose Bengal dye from waste water onto modified biomass. *Scientific Reports*, 13(1), 14776. <https://doi.org/10.1038/s41598-023-41747-5>
- [29] Shimi, A. K., Ahmed, H. M., Wahab, M., Snehlata, K., Wabaidur, S. M., Eldesoky, G. E., Islam, M. A., Rane, K. P. (2022). Synthesis and applications of green synthesized TiO<sub>2</sub> nanoparticles for photocatalytic dye degradation and antibacterial activity. *Journal of Nanomaterials*, 2022(1), 7060388. <https://doi.org/10.1155/2022/7060388>
- [30] Ajmal, A., Majeed, I., Malik, R. N., Idriss, H., Nadeem M.A. (2014). Principles and mechanisms of photocatalytic dye degradation on TiO<sub>2</sub> based photocatalysts: a comparative overview. *RSC Adv*, 4, 37003–37026. <https://doi.org/10.1039/C4RA06658H>